IEEE Access
Multidisciplinary | Rapid Review | Open Access Journal

Received March 7, 2022, accepted March 17, 2022, date of publication March 22, 2022, date of current version March 28, 2022.

Digital Object Identifier 10.1109/ACCESS.2022.3161486

Wide-Range Light Harvesting Module for Autonomous Sensor Nodes

KONSTANTINOS KOZALAKIS, (Graduate Student Member, IEEE), IOANNIS SOFIANIDIS, (Graduate Student Member, IEEE), VASILIKI GOGOLOU, (Graduate Student Member, IEEE), VASILEIOS KONSTANTAKOS, KOSTAS SIOZIOS, (Member, IEEE), STYLIANOS SISKOS, (Senior Member, IEEE), AND THEODORE LAOPOULOS, (Senior Member, IEEE)

Electronics Laboratory, Physics Department, Aristotle University of Thessaloniki, 54124 Thessaloniki, Greece

Corresponding author: Konstantinos Kozalakis (kkozalak@physics.auth.gr)

This work was supported in part by the European Regional Development Fund of the European Union and Greek National Funds through the Operational Program Competitiveness, Entrepreneurship, and Innovation, under the Call RESEARCH—CREATE—INNOVATE under Project T1EΔK-00360.

ABSTRACT A large number of autonomous devices is nowadays supported by renewable and green energy sources. A vital sub-circuit in such systems is the power converter circuit, which should efficiently transform and store the available energy. In order to obtain the maximum efficiency under varying energy conditions, various maximum power point tracking (MPPT) methods are used. In this work a complete harvesting module with battery management and MPPT is presented, suitable for a plethora of autonomous applications. A novel, low-complexity and ultra-low power consumption design is proposed, which offers very wide operating voltage and power range with high MPPT efficiency and very low power consumption. It can be combined with different harvesters, such as thermoelectric generators or photovoltaic panels and is able to work under widely varying energy conditions. As supported by experimental results, the proposed module covers a very wide working input power range, from 40 μW up to 4 W, as well as a very wide input voltage range, from 650 mV up to 2.8 V with 96.5% average MPPT efficiency and a total power consumption of 3.9 μW at 3.6 V. The module relies on an embedded ultra-low power microcontroller unit (MCU) to perform the power management and MPPT operations, which can also be used for extra tasks (e.g., sensor reading). Using the proposed module, an autonomous sensor node was built, able to acquire acceleration measurements, and wirelessly communicate with a remote user in order to send an alert or stream the acquired sensor data in real time.

INDEX TERMS Autonomous sensors, DC-DC converter, digital-to-analog converter, energy harvesting, indoor-outdoor light, Internet of Things, low-power, maximum power point tracking, self-oscillating, wide range.

I. INTRODUCTION

Energy harvesting circuits attract much interest in many autonomous applications, including portable IoT nodes and wireless sensor networks [1], [2]. Nowadays, electronic devices performing complicated tasks consume tiny amounts of energy and their undisrupted operation can be supported by harnessing ambient energy from low power sources, such as ambient radiofrequencies (RF) [3], [4], heat [5], indoor/outdoor light [6], [7], the soil [8], [9], as well as triboelectric or piezoelectric materials [10]–[13]. Usually, the power output of such sources is neither constant, nor stable. Thus, a dedicated harvesting circuit is required to efficiently transform the output power of the harvester before it can be used or stored [14], [15]. Important considerations during the design of such a circuit are its power consumption, its power conversion efficiency, as well as its operating voltage and power range [16].

To increase the power conversion efficiency, the most efficient harvesting circuits perform input matching operations, in order to dynamically track and work at the maximum power point of the harvester (Maximum power point tracking – MPPT) [17]–[19]. In ultra-low power applications dynamic MPPT solutions are not viable, as they significantly

The associate editor coordinating the review of this manuscript and approving it for publication was Agustin Leobardo Herrera-May.

increase the power consumption of the harvesting circuit [20]. Under these conditions, a non-dynamic MPPT circuit is usually preferred, optimized for a specific harvester type and a specific input energy level [21]. This type of MPPT is suitable for harvesters which provide constant output power. In use cases where the available ambient energy can vary in a wide range, such as a thermoelectric harvester or a photovoltaic panel under varying energy conditions, the implementation of a dynamic MPPT circuit is essential [22], [23]. Though the most efficient dynamic MPPT techniques are too power demanding to be applied in low power applications, in recent years, simple dynamic MPPT solutions have been developed, targeting low power systems as well [24]–[26]. However, to abide to the limitations regarding low complexity and low power consumption, most implementations adopt methods which significantly restrict the operating range of the harvesting circuit in terms of power throughput.

A large amount of harvesting circuits uses width modulated pulses (PWM) to control the power converter [27], [28]. PWM controllers increase the working range of the harvesting circuit compared with non-dynamic MPPT solutions and can easily be implemented by any digital unit without the need for extra analog circuitry or high clock frequency, which would drastically increase the power consumption [29]. Unfortunately, for wide power range, very high frequency and resolution PWM signal is required, which makes this approach not suitable for low power applications. An alternative type of control relies on frequency modulated pulses (PFM). The PFM controller can effectively exploit the whole operating range of the power converter [30]. However, it significantly increases the complexity and power consumption, as it usually requires extra analog circuitry, such as voltage-controlled oscillator (VCO) or phase-locked loop (PLL) circuits.

Another restricting factor for dynamic MPPT implementation, is the requirement of a sensing element, along with the necessary circuitry, to provide feedback of the working power of the power converter. The power measure is typically calculated using voltage and current sensors at the input or the output of the converter [31], [32]. Voltage sensing does not interfere with the operation of the converter, but on the other hand current sensing usually does [33]. The easiest and most widely used current sensing technique that relies on a sensing resistor is not suitable for applications targeting wide working range, as the voltage drop on the sensing resistor increases with the input power, leading to huge power losses. The use of a sensing resistor can be avoided using a resistor-free time-based power sensing method [34], [35]. However, this method usually requires extra analog circuitry, for instance current mirrors, capacitors, or oscillators, which also significantly increase the complexity and power consumption.

In this work the design of a low power harvesting module with MPPT and battery management is presented. It is optimized towards maximum operating voltage and power range and offers high efficiency and very low power consumption. The design is based on a wide range self-oscillating boost converter (SOB) described in a previous work [36], which automatically operates in a PFM similar way, eliminating the need for separate analog circuitry (e.g., VCO). Additionally, the use of the SOB converter eliminates the need for a separate power sensor, as the working power measurement is accurately calculated using the oscillating frequency of the SOB converter as feedback (time-based sensing), rendering the need for both voltage and current sensing unnecessary. The above advantages, significantly reduce the complexity of the MPPT controller, as there is no need for high frequency pulse control, but for voltage control instead. Voltage control is implemented by an ultra-low power microcontroller (MCU) and a custom-made nano-power digital-to-analog-converter (DAC). The MCU controls the SOB converter and performs MPPT with a minimal power consumption. The proposed harvesting module achieves a very wide operating power range from 40 μW up to 4 W and a very wide operating voltage range from 650 mV up to 2.8 V, with 96.5% average MPPT efficiency and an ultra-low power consumption of 3.9 μW at 3.6 V. These specifications allow it to work with either a thermoelectric generator, or a photovoltaic panel, and efficiently perform under widely varying energy conditions. In this work it is combined with a 68.5 cm^2 5-cell PV panel, which allows it to work both at indoor and outdoor light.

Using the proposed harvesting module an autonomous sensor node was built. The node is using the embedded MCU to additionally interface a micro-electromechanical accelerometer (MEMS technology), as well as an RF communication unit. It is able to monitor the mechanical stress in sensitive structures (e.g., industrial equipment, vehicles, bridges, buildings etc.) and remotely notify the user whenever they are under extreme stress [37]. The node can also remotely stream the acceleration data, based on which the extreme stress is defined. An indicative usage of such a feature is the measurement of the seismic response of a structure during an earthquake [38]. Furthermore, the node can be utilized in a wide range of trending applications that acquire accelerometer samples on demand. In particular, it can be used in pipeline leak detection and localization applications, which also rely on accelerometer sensors [39], [40].

The following section gives a brief description of the hardware design. In Section III the time-based resistor-free output power calculation method, as well as the MCU software that calculates the output power and performs MPPT are presented. Section IV includes all the technical information for building the prototype harvesting module. The experimental results are collected in Section V and additionally, the proposed module is compared with other state-of-the-art harvesting circuits. Section VI demonstrates the autonomous sensor node prototype, and finally, Section VII concludes this work.

II. DESIGN OF THE PROPOSED HARVESTING MODULE

In this work the design of a complete harvesting module with MPPT and battery management is presented. The design is

based on a wide power range SOB converter to charge a rechargeable battery, which automatically adjusts its oscillating frequency with the input power. The converter is automatically operating similar to a PFM controlled converter, eliminating the need for high frequency pulse control, while its input impedance can be externally controlled through an analog voltage input. Additionally, the use of the SOB converter eliminates the need for a separate power sensor, as the working power measurement can be accurately calculated using the oscillating frequency of the SOB converter as feedback (time-based sensing). This significantly reduces the complexity of the proposed harvesting module. To control the SOB converter and perform MPPT only an MCU and a DAC module are used (Fig 1).

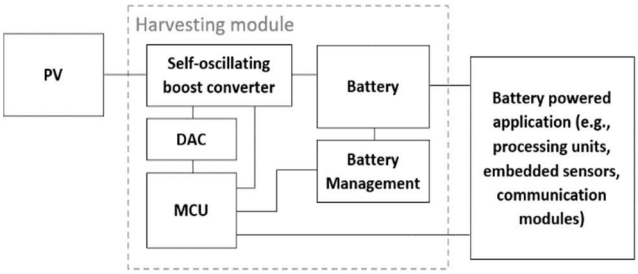

FIGURE 1. Block diagram of the proposed harvesting module.

The embedded MCU is measuring the oscillating frequency of the SOB converter, in order to calculate the output power. Additionally, it is using the DAC module to control the input impedance of the SOB converter and perform the MPPT. Moreover, the MCU is supervising the battery voltage using an internal analog-to-digital converter (ADC) and is able to discharge it through a resistive load in case of overcharging. The MPPT and battery management operations require an insignificant amount of computational power, as they are performed at a very low rate. Thus, the embedded MCU can also be used for extra tasks, depending on the use case application.

A. SELF-OSCILLATING BOOST CONVERTER

The SOB converter (Fig 2) uses an analog comparator (COMP) in order to force an externally applied reference voltage (V_{ref}) on the input capacitor (C).

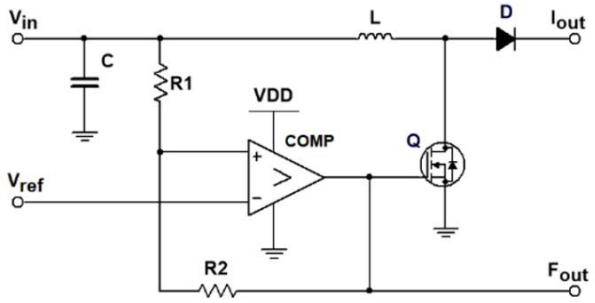

FIGURE 2. Self-oscillating boost converter's conversion efficiency versus the input power, for different voltage reference values.

The comparator produces a high voltage pulse each time a fraction of the capacitor's voltage exceeds the reference voltage, to drive the low side switch (Q) and discharge the capacitor through the inductor (L). The converter operates automatically whenever sufficient energy is available at the input, and its input impedance can be controlled with the external voltage reference (V_{ref}). A very useful feature for MPPT applications is offered by this configuration, as the working frequency, complexity, and power consumption of the MPPT circuit are significantly reduced. Another advantage of the converter is the fact that it covers a very wide operating power range. With the components used (see Section IV) the SOB converter operates for a power range from 40 μW up to 4 W, as measured (Fig 3).

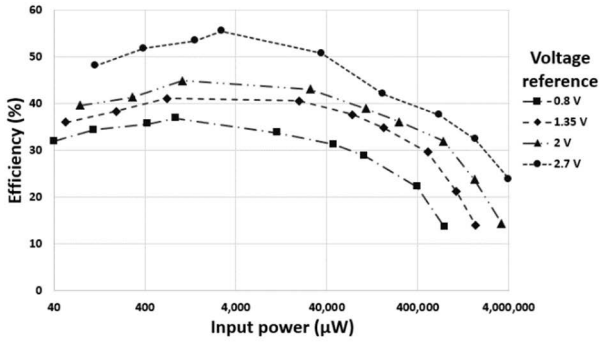

FIGURE 3. Digital-to-analog converter's schematic.

The input voltage of the SOB converter can range from 650 mV up to 2.8 V, the peak efficiency is 60% and the current consumption is as low as 100 nA.

B. DIGITAL-TO-ANALOG CONVERTER

To control the input impedance of the SOB converter and perform MPPT, an analog voltage (V_{ref}) is required. State-of-the-art of the shelf DAC units consume several μA during operation, therefore, a nano-power custom-made DAC logic was used to produce the required analog voltage, optimized for the needs of the proposed module. The custom DAC unit uses a capacitor (C1) as the output element (Fig 4).

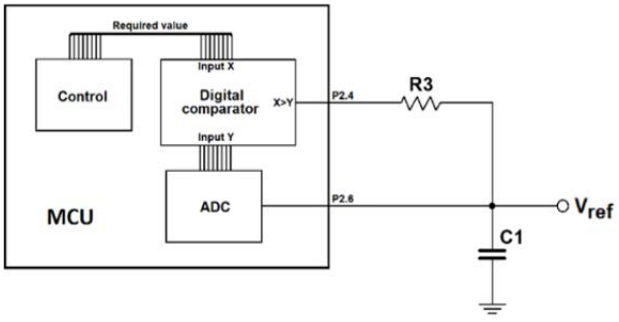

FIGURE 4. Schematic of the self-oscillating boost converter.

A general-purpose MCU can monitor the voltage of the output capacitor (C1) using an internal ADC input pin

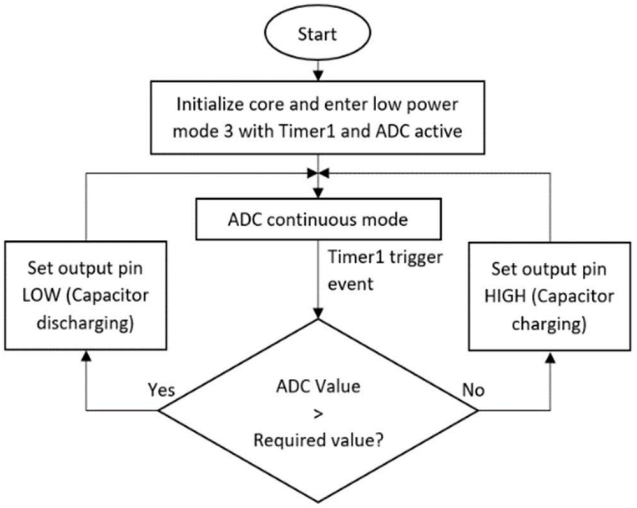

FIGURE 5. Digital-to-analog converter's control logic.

(pin 2.6). The MCU periodically measures the voltage of the capacitor using an internal timer to trigger the ADC, while being in sleep mode. Using a digital output pin (pin 2.4) the MCU can charge or discharge the output capacitor (C1) through the resistor (R3) and adjust the output voltage, in an inverted successive approximation register (SAR) logic. Fig 5 shows the flow-chart of the code running on the MCU for the DAC operation.

A small voltage ripple is observed at the output of the DAC, as the digital output pin oscillates between the charging and discharging states. The response time of the DAC, its power consumption and its output voltage ripple depend on the selected capacitor (C1) and resistor (R3) values, as well as the sampling rate of the MCU (ADC sampling rate). Since the DAC is used to perform the MPPT control, a fast response time is not required. Using a low ADC sampling rate and large resistor (R3) and capacitor (C1) values (see Section IV) the response time is approximately 100 ms for the MPPT step used and the voltage ripple is approximately 150 mV. The average current consumption of the DAC is 680 nA, including the consumption of the MCU, resulting to a significant advantage of the proposed system in terms of overall power consumption.

C. BATTERY MANAGEMENT

The implemented MCU also performs battery management operations. The MCU monitors the battery voltage using a resistor divider and an ADC input pin. If the battery is fully charged, the MCU activates a bleeder resistor to draw any excess energy and protect the battery from overcharging. Additionally, a voltage regulator is required to supply power at the MCU, as well as the SOB converter. Selecting the appropriate voltage regulator and resistor divider components, any battery or supercapacitor is supported for the energy storage, as long as the working voltage is greater than 3.3 V.

III. MAXIMUM POWER POINT TRACKING OPERATIONS

A. TIME-BASED OUTPUT POWER CALCULATION

The SOB converter (Fig 2) starts to oscillate, whenever sufficient power is applied at its input. The oscillating frequency depends on the applied voltage reference (V_{ref}), the inductance of the inductor (L), the capacitance of the input capacitor (C), the resistance values of the resistor divider (R1, R2 which are used to create a small hysteresis window), the output battery voltage, and the working power. All the above parameters excluding the external V_{ref} and working power are selected at the design phase and remain constant during the operation of the converter. Thus, for fixed V_{ref}, a fixed amount of energy will be transferred through the converter at each oscillation, and the frequency of the oscillations should be proportional to the working power of the converter. Using the DAC presented in the previous section to control the SOB converter, measurements of the oscillating frequency and the output power of the converter were obtained, for different input voltage reference values (V_{ref}) (Fig 6).

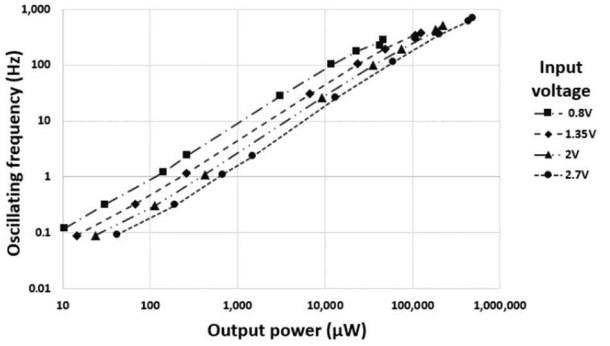

FIGURE 6. Self-oscillating boost converter's oscillation frequency.

As shown, the oscillating frequency of the SOB converter is indeed proportional to its output power for fixed voltage reference. For high working power, the response time of the comparator used for the SOB converter is comparable with the converter's oscillating frequency, increasing the input voltage ripple, and distorting the otherwise linear relationship. However, using the obtained measurements, and regression analysis tools, a function that is able to calculate the output power of the SOB converter in the whole operating range was found. Eq (1) gives the output power of the converter in μW, given the converter's oscillating frequency (F_{osc} in Hz) and applied voltage reference (V_{ref} in V).

$$p_{out} = \frac{60.9049 * V_{ref}{}^2 + 69.8622 * V_{ref} - 26.885}{F_{osc}{}^{0.047 * ln(V_{ref}) + 3.0741}} \quad (1)$$

Using Eq. (1) the MCU can calculate the output power of the SOB converter with 81% average accuracy in the whole operating voltage and power range (Fig 7).

B. MAXIMUM POWER POINT TRACKING

For the MPPT, the MCU controls the SOB converter using the DAC (See Section II) and measures the converter's oscillating

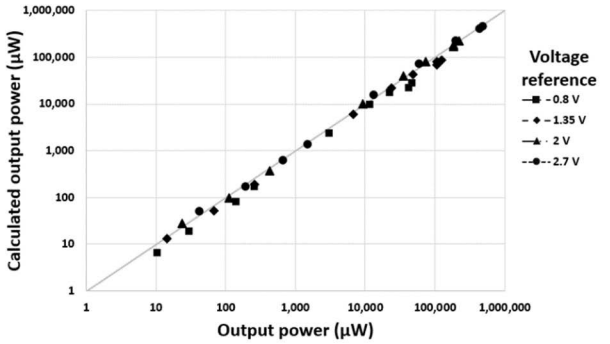

FIGURE 7. Calculated output power versus the actual output power of the self-oscillating boost converter for different voltage reference values.

FIGURE 8. Assembled printed circuit board.

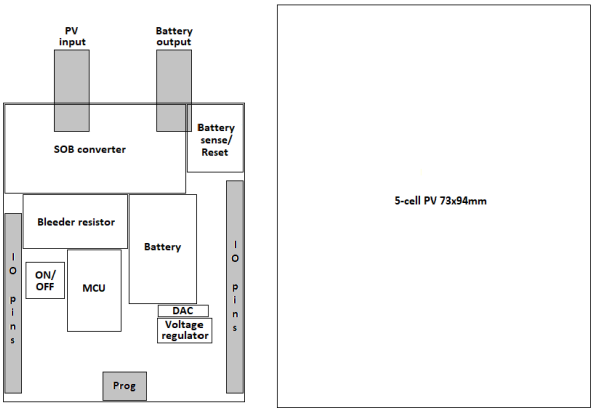

FIGURE 9. Size comparison of the units.

frequency in order to calculate the output power. As the SOB converter unit is autonomous, the main task of the MCU is to monitor the DAC. Using an external interrupt input pin (pin 1.6), the MCU is also able to count the oscillations of the SOB converter that occur within the DAC samplings. Since the DAC samplings are synchronized by an internal timer, the time period is also known, and the MCU can measure the oscillating frequency of the SOB converter. With the frequency feedback and using Eq. (1) the MCU can calculate the working power and adjust the input voltage of the SOB converter to track the MPP voltage.

The MPPT method used is based on the perturb and observe approach (P&O). However, the MCU implementation offers huge flexibility to the module considering the MPPT method selection, and various algorithms can be tested and compared. In this work, a simple P&O algorithm was implemented, offering fair performance at the lowest power consumption. A step of 65 mV was selected for the P&O algorithm and the MCU performs an output power calculation every 10 seconds. This increases the average current consumption of the MCU from 400 nA (idle state) to 5 μA during the MPPT operation (active state). The above configuration offers fair optimization between the power consumption and the efficiency of the MPPT operation.

IV. PROTOTYPE HARVESTING MODULE

A printed circuit board (PCB) was designed for the prototype, that offers all the unused MCU pins in an Arduino UNO compatible pinout. The assembled PCB and the area that each unit occupies are shown in Fig 8 and Fig 9, respectively. The size of the PCB is 53 $\times$ 68 mm, and the size of the used PV panel is 73 $\times$ 94 mm.

The proposed module relies on an ultra-low power MCU from Texas Instruments, the MSP430FR5969. The MSP430FR5969 offers an extremely low current consumption in deep sleep mode (20 nA). Additionally, it features an internal ADC, able to work autonomously in the background while the main core is at sleep mode — a feature suitable for the proposed harvesting module. Selecting a low sampling rate for the ADC, the average current consumption is as low as 400 nA (idle state). During the MPPT operation the consumption increases to 5 μA (active state).

For the battery management operations, a 1.5 Ω bleeder resistor is used, as well as a 6.8 + 6.8 MΩ resistor divider for the battery voltage sensing. The module relies on an 80 mAh 3.6 V Li-ion battery for the energy storage and a nano power LDO from Texas Instruments, the TPS7A02, is providing 3.3V regulated voltage supply to the units.

The energy harvesting (MPPT) and battery management operations do not require significant computational power and the embedded MCU can also be used for extra tasks, depending on the use-case application. The MCU is mostly at sleep mode, working for only a few hundred cycles per second to supervise the DAC and battery voltages (idle state). This allows the module to work with a minimal power consumption. If required by the use-case application, the MPPT operation can be shortly interrupted and the MCU is available to perform a critical operation (see Section VI).

The SOB converter is implemented as shown in Fig 2, using the following components: C = 3 mF, L = 1 mH, D = 1N4148, Q = PMV40UN2, U = TLV3691, R1 = 100 KΩ and R2 = 3.3 MΩ. Large capacitor (C) and inductor (L) values are used, in order to minimize the oscillating frequency and allow the converter to operate in a very wide power range. Using the

nano-power analog comparator from Texas Instruments, the TLV3691, the current consumption of the SOB converter is as low as 100 nA.

The custom-made DAC is implemented as shown in Fig 4, using the following components: R3 = 10 MΩ and C1 = 1 μF. Using a large resistor (R3) and capacitor (C1) a low sampling frequency of 2 Hz can be used, minimizing the current consumption at 680 nA, including the consumption of the MCU performing all the required actions.

Table 1 presents the power consumption of each unit at idle and active state. As shown, the total current consumption of the proposed harvesting module is 1.09 μA at idle state and 6.01 μA at active state. An ultra-low power consumption, that significantly increases the expected battery duration.

TABLE 1. Current and Power Consumption for each unit at Idle and Active state.

Unit	Idle consumption		Active consumption	
	Current	Power @3.6V	Current	Power @3.6V
MCU	400 nA	1.44 µW	5 µA	18 µW
SOB converter	100 nA	0.36 µW	100 nA	0.36 µW
DAC	280 nA	1.008 µW	280 nA	1.008 µW
Battery sensing	260 nA	0.936 µW	260 nA	0.936 µW
Voltage regulator	50 nA	0.18 µW	100 nA	0.36 µW
Total	1.09 µA	3.9 µW	6.01 µA	21.6 µW

V. EXPERIMENTAL RESULTS

The proposed harvesting module was tested for different input power values and different working voltages, using a voltage source with a series connected resistor to provide power at the input. In this setup the MPP voltage that should appear at the input of the harvesting module is half the value of the voltage source's voltage (V_{source}). Using different voltage source (V_{source}) and series resistor (R_{series}) configurations, the module was tested for the whole operating voltage and power range. Figure 10 shows the input voltage (Channel 1 top) as well as the digital-to-analog converter's voltage (Channel 2 bottom), during the operation of the harvesting module.

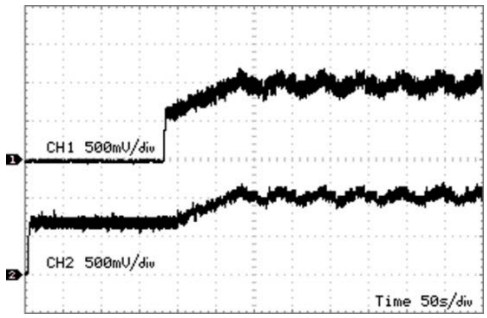

FIGURE 10. Maximum power point tracking efficiency and end-to-end efficiency versus the input power for different input voltage values.

Initially, there is no power at the input (V_{source} = 0 V) and the initial DAC output is the lowest working voltage (650 mV). Afterwards, the voltage source is set at 1.8 V with a 2 KΩ resistor connected in series (R_{series} = 2 KΩ) to provide power at the input. In this setup the MPP voltage is 0.9 V. As shown, during the P&O operation the input voltage oscillates between 760 mV and 1.2 V with an average value of 0.98 V.

Fig 11 shows the average MPPT efficiency and the average end-to-end efficiency of the proposed harvesting module. The average MPPT efficiency is 96.5% and the average end-to-end efficiency is 35% for input power ranging from 40 μW up to 4 W. The achieved end-to-end efficiency might appear low, however, taking into consideration the very wide operating range, the proposed module will be more efficient under varying energy conditions, compared with a similar implementation with greater efficiency but a more limited operating power range.

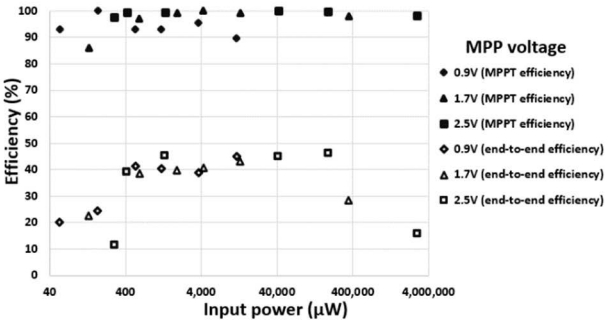

FIGURE 11. Channel 1 (Top): Input voltage; Channel 2 (Bottom): Digital-to-analog converter's outpust voltage.

Using a flexible light harvester by PowerFilm, the LL200-2.4–75 and a portable LUX meter by UNI-T, the UT383, the proposed harvesting module was evaluated for light intensities, at both indoor and outdoor conditions. The size of the PV panel is 73 × 94 mm (68.5 cm^2, 5-cell), and can provide power ranging from 60 μW in low-indoor light (60 LUX) up to 250 mW maximum in outdoor conditions (120,000 LUX). The power provided to the battery for different light intensities, taking into consideration the power consumption of the harvesting module (21.6 μW at 3.6 V during harvesting), is shown in Table 2. As shown the module is able to harness any available amount of light and can operate with a minimum amount of light of 60 LUX.

TABLE 2. Power provided to the battery for different light intensities.

Light intensity (LUX)	Charging power (µW)
60 [1]	3.3
220 [1]	79.8
500 [1]	463.3
5,000 [2]	2,000
60,000 [2]	37,100
120,000 [2]	74,000

[1] Indoor light; [2] Outdoor light

As the module can handle up to 4 W at its input, it can be combined with a more efficient PV cell and operate in wider lighting range.

Finally, in Table 3, this work is compared with other state-of-the-art harvesting circuits. As shown, the proposed module achieves the widest operating power range between the similar state-of-the-art works, with average efficiency. Additionally, it performs with very low power consumption that makes it suitable for ultra-low power autonomous applications.

TABLE 3. Harvesting module's performance summary and comparison.

Ref no.	Technology	MPPT efficiency	Power range	Idle consumption
[17]	0.18µm	98%	0.033 – 1.2 mW	9 µW
[19]	0.18µm	86%	0 – 21 µW	12 µW
[23] [1]	Discrete	99.75%	0.01 – 300 mW	73.5 µW
[29]	0.35µm	99.9%	0.4 – 21.1 W	10.65 mW
[34]	65nm	96.2%	6 – 600 µW	5.1 µW
This work	Discrete	96.5%	40 µW – 4 W	3.9 µW

[1] Previous work

VI. PROTOTYPE AUTONOMOUS SENSOR NODE

The indoor-outdoor light harvesting module described in this work can support a plethora of applications and be combined with a wide range of PV panels and storage media. For demonstration purposes, a prototype autonomous sensor node was developed. The construction fits inside an enclosure box with 73 × 94 × 35 mm external dimensions. The node can be attached on structures of any size, such as industrial equipment, vehicles, bridges, buildings, or any other sensitive structure, and using a MEMS accelerometer sensor it can supervise the vibration and acceleration stress they are under. Also, with an RF transceiver unit it can either send a single alert message whenever the structure is under extreme stress (e.g., during an earthquake), or remotely stream the acquired sensor data. The acceleration data can be used to measure the seismic response of a building or a bridge during an earthquake, but also for many other purposes (e.g., pipeline leak detection and localization applications).

The harvesting module uses the components mentioned in Section IV, as well as the 73 × 94 mm (68.5 cm^2, 5-cell) PV panel mentioned in Section V. The autonomous sensor node relies on the existing MCU of the harvesting module, to also interface a nano-power consumption accelerometer from Analog Devices, the model ADXL362, as well as an RF transceiver by Texas Instruments, the CC2500. The ADXL362 accelerometer can monitor the acceleration in three axes while consuming only 270 nA (in ultra-low power mode) and has the ability to trigger the MCU if the acceleration at any axis exceeds a user defined threshold level. During measuring, the current consumption of the accelerometer increases to 1.8 μA (100 Hz data sampling rate). The CC2500 RF transceiver is a low power wireless communication unit with a range up to 20 meters. The idle current consumption is 400 nA and the active current consumption is as low as 12 mA.

The overall power consumption of the node is 6.3 μW at 3.6 V (idle mode), including the consumptions of the accelerometer in trigger mode and the RF transceiver in idle mode. If a change in the acceleration is detected, the MCU can acquire and process the acceleration measurements locally (measuring mode) and/or activate the RF transceiver and send an alert to a nearby receiver (alert transmission mode). The transmission duration of a single alert is approximately 1.57 ms, and during this period, the power consumption is 43.4 mW. Moreover, the actual acceleration measurements can be transmitted (data transmission mode).

For 1 minute acceleration measuring and data transmission, the node requires 1 minute in measuring mode and approximately 1.3 s in transmission mode. The average power consumption for continuous acceleration measuring and transmission is 1.5 mW. Using a fully charged, 3.6 V, 80 mAh battery, the node can send more than 15 million alerts or continuously stream the acceleration measurements for more than 7 days without any available light energy. Table 4 shows the power consumption of the proposed sensor node in different working modes.

TABLE 4. Power consumption for the different working modes.

Power consumption at 3.6 V			
Unit	Trigger mode	Measuring mode	Transmission mode
Harvesting module	3.9 µW	180 µW	180 µW
Accelerometer	0.97 µW	6.48 µW	0.97 µW
RF transceiver	1.44 µW	1.44 µW	43.2 mW
Total	6.3 µW	187.9 µW	43.4 mW

TABLE 5. Expected battery duration for different lighting conditions and no detected acceleration stress per day.

Battery duration in **years** (3.6V 80mAh Li-ion)				
Light intensity (LUX)	Charging time duration per day			
	1min	1hour	3hours	6hours
0	1.26	1.26	1.26	1.26
60 [1]	1.26	1.32	1.46	1.75
220 [1]	1.27	2.45	Inf [3]	Inf [3]
500 [1]	1.32	Inf [3]	Inf [3]	Inf [3]
5,000 [2]	1.56	Inf [3]	Inf [3]	Inf [3]
60,000 [2]	Inf [3]	Inf [3]	Inf [3]	Inf [3]
120,000 [2]	Inf [3]	Inf [3]	Inf [3]	Inf [3]

[1] Indoor light; [2] Outdoor light; [3] Battery remains infinitely charged

Table 5 shows the expected battery duration for different lighting conditions, in case of no detected acceleration stress. With a minimum of 220 LUX of indoor light available for only 2.5 hours per day, the expected battery duration is infinite.

Finally, Table 6 shows the expected battery duration for different lighting conditions in case of 4,000 detected alerts or an average of 2.7 minutes of acceleration measuring per day. The above is an extreme scenario regarding the

TABLE 6. Expected battery duration for different lighting conditions and 4,000 alerts or 2.7 minutes of acceleration measuring per day.

Battery duration in **years** (3.6V 80mAh Li-ion)				
Light intensity (LUX)	Charging time duration per day			
	1min	1hour	3hours	6hours
0	0.88	0.88	0.88	0.88
60 [1]	0.88	0.92	1.01	1.2
220 [1]	0.88	1.35	Inf [3]	Inf [3]
500 [1]	0.90	Inf [3]	Inf [3]	Inf [3]
5,000 [2]	1.01	Inf [3]	Inf [3]	Inf [3]
60,000 [2]	Inf [3]	Inf [3]	Inf [3]	Inf [3]
120,000 [2]	Inf [3]	Inf [3]	Inf [3]	Inf [3]

[1] Indoor light; [2] Outdoor light; [3] Battery remains infinitely charged

working time duration, since the proposed node is targeted for the monitoring of extreme stress conditions that sparsely occur (e.g., earthquake or pipeline leak). As shown, the life expectancy of the node is infinite for a minimum amount of light of 220 LUX (home indoor) available for 3 hours per day, or 120,000 LUX (sunny outdoor) available for only a few seconds per day. The battery duration is extended by 36% with a minimum amount of light of 60 LUX available for 6 hours per day.

VII. CONCLUSION

A complete energy harvesting module with MPPT and battery management has been presented in this work. The module is optimized for light energy harvesting both at indoor and outdoor conditions and covers a very wide input power range, from 40 μW up to 4 W, as well as a very wide input voltage range, from 650 mV up to 2.8 V. The proposed module is optimized for use with a PV panel consisting of 2 up to 5 cells with a maximum output power of 4 W and can be combined with any battery or supercapacitor for the energy storage with a working voltage greater than 3.3 V. Using an ultra-low power MCU it performs MPPT with 96.5% average efficiency and 35% average end-to-end efficiency. The MCU can also be used for extra tasks and the proposed module is a powerful tool for a wide variety of autonomous ultra-low power applications with an idle power consumption of 3.9 μW at 3.6 V.

Using the proposed harvesting module, a prototype autonomous sensor node was designed in this work. The node can supervise the mechanical stress of structures, such as bridges, buildings, or sensitive industrial installations of smaller or bigger scale and remotely notify the user in case of excess vibration or acceleration stress detection. Also, the node can wirelessly transmit the acceleration data if required. Using a 68.5 cm^2 5-cell PV panel and a small size 80 mAh 3.6 V Li-ion battery, the life expectancy of the sensor node is infinite both at outdoor and indoor conditions.

REFERENCES

[1] A. Omairi, Z. H. Ismail, K. A. Danapalasingam, and M. Ibrahim, "Power harvesting in wireless sensor networks and its adaptation with maximum power point tracking: Current technology and future directions," *IEEE Internet Things J.*, vol. 4, no. 6, pp. 2104–2115, Dec. 2017.

[2] T. Sanislav, G. D. Mois, S. Zeadally, and S. C. Folea, "Energy harvesting techniques for Internet of Things (IoT)," *IEEE Access*, vol. 9, pp. 39530–39549, 2021.

[3] D. Khan, S. J. Oh, K. Shehzad, M. Basim, D. Verma, Y. G. Pu, M. Lee, K. C. Hwang, Y. Yang, and K.-Y. Lee, "An efficient reconfigurable RF-DC converter with wide input power range for RF energy harvesting," *IEEE Access*, vol. 8, pp. 79310–79318, 2020.

[4] S. M. Noghabaei, R. L. Radin, Y. Savaria, and M. Sawan, "A high-sensitivity wide input-power-range ultra-low-power RF energy harvester for IoT applications," *IEEE Trans. Circuits Syst. I, Reg. Papers*, vol. 69, no. 1, pp. 440–451, Jan. 2022.

[5] L. Liu, Y. Xing, W. Huang, X. Liao, and Y. Li, "A 10 mV-500 mV input range, 91.4% peak efficiency adaptive multi-mode boost converter for thermoelectric energy harvesting," *IEEE Trans. Circuits Syst. I, Reg. Papers*, vol. 69, no. 2, pp. 609–619, Feb. 2022.

[6] F. Mateen, M. A. Saeed, J. W. Shim, and S.-K. Hong, "Indoor/outdoor light-harvesting by coupling low-cost organic solar cell with a luminescent solar concentrator," *Sol. Energy*, vol. 207, pp. 379–387, Sep. 2020.

[7] D. Bol, E. H. Boufouss, D. Flandre, and J. De Vos, "A 0.48 mm^2 5μW-10 mW indoor/outdoor PV energy-harvesting management unit in a 65 nm SoC based on a single bidirectional multi-gain/multi-mode switched-cap converter with supercap storage," in *Proc. 41st Eur. Solid-State Circuits Conf. (ESSCIRC)*, Sep. 2015, pp. 241–244.

[8] I.-C. Ou, J.-P. Yang, C.-H. Liu, K.-J. Huang, K.-J. Tsai, Y. Lee, Y.-H. Chu, and Y.-T. Liao, "A sustainable soil energy harvesting system with wide-range power-tracking architecture," *IEEE Internet Things J.*, vol. 6, no. 5, pp. 8384–8392, Oct. 2019.

[9] M. Bhuyian, M. Al-Tekreeti, K. Naik, B. Plourde, and G. Sakauye, "A soil-based energy harvester for wireless sensor nodes to monitor corrosion characteristics of underground water pipes," in *Proc. IEEE SENSORS*, Oct. 2019, pp. 1–4.

[10] A. A. Khan, A. Mahmud, and D. Ban, "Evolution from single to hybrid nanogenerator: A contemporary review on multimode energy harvesting for self-powered electronics," *IEEE Trans. Nanotechnol.*, vol. 18, pp. 21–36, 2019.

[11] Y. Hu, A. Luo, J. Wang, and F. Wang, "Voltage regulation and power management for wireless flow sensor node self-powered by energy harvester with enhanced reliability," *IEEE Access*, vol. 7, pp. 154836–154843, 2019.

[12] B. Ciftci, S. Chamanian, A. Koyuncuoglu, A. Muhtaroglu, and H. Kulah, "A low-profile autonomous interface circuit for piezoelectric micro-power generators," *IEEE Trans. Circuits Syst. I, Reg. Papers*, vol. 68, no. 4, pp. 1458–1471, Apr. 2021.

[13] H. Liu, J. Zhong, C. Lee, S.-W. Lee, and L. Lin, "A comprehensive review on piezoelectric energy harvesting technology: Materials, mechanisms, and applications," *Appl. Phys. Rev.* vol. 5, no. 4, 2018, Art. no. 041306.

[14] X. Yue, M. Kauer, M. Bellanger, O. Beard, M. Brownlow, D. Gibson, C. Clark, C. MacGregor, and S. Song, "Development of an indoor photovoltaic energy harvesting module for autonomous sensors in building air quality applications," *IEEE Internet Things J.*, vol. 4, no. 6, pp. 2092–2103, Dec. 2017.

[15] D. Newell and M. Duffy, "Review of power conversion and energy management for low-power, low-voltage energy harvesting powered wireless sensors," *IEEE Trans. Power Electron.*, vol. 34, no. 10, pp. 9794–9805, Oct. 2019.

[16] A. M. George and S. Y. Kulkarni, "Performance of power converters for ultra low power systems: A review," in *Proc. 2nd Int. Conf. Adv. Electron., Comput. Commun. (ICAECC)*, Bengaluru, India, Feb. 2018, pp. 1–5.

[17] L. Liu, C. Huang, J. Mu, J. Cheng, and Z. Zhu, "A P&O MPPT with a novel analog power-detector for WSNs applications," *IEEE Trans. Circuits Syst. II, Exp. Briefs*, vol. 67, no. 10, pp. 1680–1684, Oct. 2020.

[18] R. B. Bollipo, S. Mikkili, and P. K. Bonthagorla, "Hybrid, optimal, intelligent and classical PV MPPT techniques: A review," *CSEE J. Power Energy Syst.*, vol. 7, no. 1, pp. 9–33, Jan. 2021.

[19] X. Liu and E. Sanchez-Sinencio, "An 86% efficiency 12 μW self-sustaining PV energy harvesting system with hysteresis regulation and time-domain MPPT for IoT smart nodes," *IEEE J. Solid-State Circuits*, vol. 50, no. 6, pp. 1424–1437, Jun. 2015.

[20] A. Paidimarri and A. P. Chandrakasan, "A wide dynamic range buck converter with sub-nW quiescent power," *IEEE J. Solid-State Circuits*, vol. 52, no. 12, pp. 3119–3131, Dec. 2017.

[21] W. Harmon, D. Bamgboje, H. Guo, T. Hu, and Z. L. Wang, "Self-driven power management system for triboelectric nanogenerators," *Nano Energy*, vol. 71, May 2020, Art. no. 104642.
[22] S. Kouridakis and P. Giakoumakis, "Electronic device design for energy harvesting of indoor and outdoor light sources for multiple low power usage," *Int. J. Circuits Electron.*, vol. 5, pp. 49–54, Jul. 2020.
[23] K. Kozalakis, I. Sofianidis, V. Konstantakos, K. Siozios, and S. Siskos, "73.5 uW indoor-outdoor light harvesting system with global maximum power point tracking," *J. Low Power Electron. Appl.*, vol. 11, no. 1, p. 10, Feb. 2021.
[24] S. C. Chandrarathna and J.-W. Lee, "A dual-stage boost converter using two- dimensional adaptive input-sampling MPPT for thermoelectric energy harvesting," *IEEE Trans. Circuits Syst. I, Reg. Papers*, vol. 66, no. 12, pp. 4888–4900, Dec. 2019.
[25] S. Mondal and R. Paily, "On-chip photovoltaic power harvesting system with low-overhead adaptive MPPT for IoT nodes," *IEEE Internet Things J.*, vol. 4, no. 5, pp. 1624–1633, Oct. 2017.
[26] M.-C. Chang and S.-I. Liu, "An indoor photovoltaic energy harvester using time-based MPPT and on-chip photovoltaic cell," *IEEE Trans. Circuits Syst. II, Exp. Briefs*, vol. 67, no. 11, pp. 2432–2436, Nov. 2020.
[27] C. Shi, B. Miller, K. Mayaram, and T. Fiez, "A multiple-input boost converter for low-power energy harvesting," *IEEE Trans. Circuits Syst. II, Exp. Briefs*, vol. 58, no. 12, pp. 827–831, Dec. 2011.
[28] A. A. Abdelmoaty, M. Al-Shyoukh, Y. Hsu, and A. A. Fayed, "A MPPT circuit with 25μW power consumption and 99.7% tracking efficiency for PV systems," *IEEE Trans. Circuits Syst. I, Reg. Papers*, vol. 64, no. 2, pp. 272–282, Feb. 2017.
[29] S. Uprety and H. Lee, "A 43 V 400 mW-to-21W global-search-based photovoltaic energy harvester with 350μs transient time, 99.9% MPPT efficiency, and 94% power efficiency," in *IEEE ISSCC Dig. Tech. Papers*, San Francisco, CA, USA, Feb. 2014, pp. 404–405.
[30] P.-H. Chen, H.-C. Cheng, Y.-A. Ai, and W.-T. Chung, "Automatic mode-selected energy harvesting interface with >80% power efficiency over 200 nW to 10 mW," *IEEE Trans. Very Large Scale Integr. (VLSI) Syst.*, vol. 26, no. 12, pp. 2898–2906, Dec. 2018.
[31] C.-S.-A. Gong and L.-X. Chang, "A wide-range charge controller for solar sensor," *J. Circuits, Syst. Comput.*, vol. 24, no. 7, Aug. 2015, Art. no. 1550108.
[32] S. Uprety and H. Lee, "A 0.4 W-to-21 W fast-transient global-search-algorithm based integrated photovoltaic energy harvester with 99% GMPPT efficiency and 94% power efficiency," *IEEE J. Solid-State Circuits*, vol. 51, no. 9, pp. 2153–2167, Sep. 2016.
[33] T.-W. Hsu, H.-H. Wu, D.-L. Tsai, and C.-L. Wei, "Photovoltaic energy harvester with fractional open-circuit voltage based maximum power point tracking circuit," *IEEE Trans. Circuits Syst. II, Exp. Briefs*, vol. 66, no. 2, pp. 257–261, Feb. 2019.
[34] K. Rawy, F. Kalathiparambil, D. Maurath, and T. T. Kim, "A self-adaptive time-based MPPT with 96.2% tracking efficiency and a wide tracking range of 10 μ A to 1 mA for IoT Applications," *IEEE Trans. Circuits Syst. I, Reg. Papers*, vol. 64, no. 9, pp. 2334–2345, Sep. 2017.
[35] S.-H. Wu, X. Liu, Q. Wan, Q. Kuai, Y.-K. Teh, and P. K. T. Mok, "A 0.3-V ultralow-supply-voltage boost converter for thermoelectric energy harvesting with time-domain-based MPPT," *IEEE Solid-State Circuits Lett.*, vol. 4, pp. 100–103, 2021.
[36] K. Kozalakis and S. Siskos, "Design of a self-oscillating DC-DC boost converter with constant efficiency in a wide power range for energy harvesting applications," in *Proc. Panhellenic Conf. Electron. Telecommun. (PACET)*, Volos, Greece, Nov. 2019, pp. 1–4.
[37] M. J. Whelan, M. V. Gangone, and K. D. Janoyan, "Highway bridge assessment using an adaptive real-time wireless sensor network," *IEEE Sensors J.*, vol. 9, no. 11, pp. 1405–1413, Nov. 2009.
[38] T. Torfs, T. Sterken, S. Brebels, J. Santana, R. van den Hoven, V. Spiering, N. Bertsch, D. Trapani, and D. Zonta, "Low power wireless sensor network for building monitoring," *IEEE Sensors J.*, vol. 13, no. 3, pp. 909–915, Mar. 2013.
[39] M.-U.-R.-A. Virk, M. F. Mysorewala, L. Cheded, and I. M. Ali, "Leak detection using flow-induced vibrations in pressurized wall-mounted water pipelines," *IEEE Access*, vol. 8, pp. 188673–188687, 2020.
[40] G.-P. Kousiopoulos, G.-N. Papastavrou, D. Kampelopoulos, N. Karagiorgos, and S. Nikolaidis, "Comparison of time delay estimation methods used for fast pipeline leak localization in high-noise environment," *Technologies*, vol. 8, no. 2, p. 27, May 2020.

KONSTANTINOS KOZALAKIS (Graduate Student Member, IEEE) received the B.Sc. degree in physics, in 2014, and the M.Sc. degree in electronic physics—radioelectrology from the Department of Physics, Aristotle University of Thessaloniki, in 2017. He is currently pursuing the Ph.D. degree, working on the design of electronic circuits and systems for energy harvesting and measurements. His research interests include analog and mixed signal circuit design for biological and medical applications.

IOANNIS SOFIANIDIS (Graduate Student Member, IEEE) received the M.Sc. degree in electronic physics (radioelectrology) from the Physics Department, Aristotle University of Thessaloniki, Greece, in 2020. He is currently pursuing the Ph.D. degree. During his M.Sc. degree, he participated in the development of a low power mems accelerograph for strong motion seismic activity monitoring. His research interests include estimation and reduction techniques regarding energy consumption in electronic systems.

VASILIKI GOGOLOU (Graduate Student Member, IEEE) received the B.Sc. degree in physics and the M.Sc. degree in electronic physics (radioelectrology) from the Physics Department, Aristotle University of Thessaloniki, in 2016 and 2019, respectively. She is currently pursuing the Ph.D. degree. Her research interests include low-power integrated circuits design for energy harvesting and the IoT applications.

VASILEIOS KONSTANTAKOS received the Ph.D. degree from the Department of Physics, Aristotle University of Thessaloniki, Greece, in 2010. He is currently a Postdoctoral Researcher with the Aristotle University of Thessaloniki. His research interests include the development of electronic instrumentation systems, targeting various characteristics like automation, increased functionality, high portability, and low energy consumption. He participated in various research programs with instrumentation challenges in different research areas, like in classical electronics, nuclear physics, and athletics science.

KOSTAS SIOZIOS (Member, IEEE) received the Diploma, master's, and Ph.D. degrees in electrical and computer engineering from the Democritus University of Thrace, Greece, in 2001, 2003, and 2009, respectively. He is currently an Assistant Professor with the Department of Physics, Aristotle University of Thessaloniki. The last years, he works as the Project Coordinator, and the Technical Manager or the Principal Investigator in numerous research projects funded from the European Commission (EC), European Space Agency (ESA), and the Greek Government and Industry. He has published more than 130 papers in peer-reviewed journals and conferences. He has also contributed to five books of Kluwer and Springer. His research interests include low-power hardware accelerators, resource allocation, machine learning, decision-making algorithms, cyber-physical systems (CPS), and the IoT for smart-grid.

STYLIANOS SISKOS (Senior Member, IEEE) was born in 1956. He received the B.Sc. degree in physics from the Aristotle University of Thessaloniki, Thessaloniki, Greece, in 1980, and the M.Sc. and Ph.D. degrees in electronics from the University of Paul Sabatier de Toulouse, Toulouse, France, in 1983. He was a Lecturer with the Polytechnic School, Thessaloniki, from 1985 to 1989. In 1989, he joined the Electronics Laboratory, Physics Department, Aristotle University of Thessaloniki, as a Lecturer, where he is currently a Professor. His current research interests include analog and mixed signal integrated-circuit design, mixed built-in signal structures, current-mode integrated-circuit design, sensor-interfacing integrated circuits, design of signal-processing circuits, and low-voltage analog integrated circuits for energy harvesting applications.

THEODORE LAOPOULOS (Senior Member, IEEE) received the B.Sc. degree in physics and the Ph.D. degree in control electronics from the Aristotle University of Thessaloniki, Thessaloniki, Greece, in 1980 and 1989, respectively. He is currently an Associate Professor with the Electronics Laboratory and the Academic Coordinator of the Socrates/Erasmus Program with the Department of Physics, Aristotle University of Thessaloniki. He has published more than 100 papers in international scientific journals and conference proceeding papers and has served as a Coordinator in 12 Greek and European research projects and a Senior Researcher in others. His research interests include instrumentation circuits and systems, measurement systems and techniques, sensor interfacing, automation, applications of microcontroller systems, and education on electronic instrumentation. He is an Associate Editor of the IEEE TRANSACTIONS ON INSTRUMENTATION AND MEASUREMENT and the Chair of the Advisory Board of the IDAACS International Workshop on Intelligent Data Acquisition and Advanced Computing Systems.